**Discover** Nano

Review

# Hydrogen sensors based on polyaniline and its hybrid materials: a mini review

**Perizat Askar**[1] · **Dana Kanzhigitova**[1] · **Aslan Tapkharov**[2] · **Kamshat Umbetova**[3,4] · **Sagydat Duisenbekov**[1] · **Salimgerey Adilov**[2] · **Nurxat Nuraje**[1,4]

Received: 16 September 2024 / Accepted: 3 March 2025

**Abstract**
This mini-review examines the potential of polyaniline (PANI) composites in hydrogen sensing applications, emphasizing the mechanisms underlying PANI-hydrogen interactions. It highlights the properties and synthesis methods of different nanostructured pure PANI, PANI-carbon-based composites, and PANI-metal oxide-based composites, emphasizing approaches and PANI's hydrogen sensing performance. The review explores the electrical and morphological properties of PANI and different hybrid materials' nanocomposites, focusing on their enhanced sensitivity in hydrogen detection. Additionally, it addresses challenges such as poor solubility and low thermal stability, while outlining future research directions to advance this critical field.

**Keywords** Polyaniline · Hydrogen sensor · Nanomaterials · Conducting polymer

## 1 Introduction

Hydrogen, the lightest element in the universe, has immense potential as a sustainable and green energy source. Its ability to act as a carbon-free alternative to fossil fuels positions hydrogen as a pivotal contributor to achieving net-zero emissions by mid-century. When combined with fuel cell technology, hydrogen can serve as a reliable energy source [1, 2]. However, its high flammability, with ignition possible at concentrations as low as 4% in air, underscores the critical need for early detection of hydrogen leaks during storage and transportation [1, 3].

As a conducting polymer (CP), Polyaniline (PANI) has garnered significant attention for its diverse applications across various fields, primarily due to its unique electrical properties, environmental stability, and ease of synthesis [4, 5]. It is prominently employed in sensors [6–9], where its high sensitivity allows for the detection of gases [10–12], biomolecules [13], and other chemical species [14]. In the realm of energy storage [15, 16], PANI is used in supercapacitors and batteries, enhancing charge storage capabilities thanks to its excellent conductivity [17]. Additionally, its mechanical flexibility makes it suitable for flexible displays, wearable electronics, and electrochromic devices [18]. Furthermore, it serves as an effective antistatic coating to protect sensitive electronic components from static electricity [19, 20].

---

✉ Nurxat Nuraje, nurxat.nuraje@nu.edu.kz; Salimgerey Adilov, sadilov@nu.edu.kz | [1]Department of Chemical and Materials Engineering, School of Engineering and Digital Science, Nazarbayev University, 010000 Astana, Kazakhstan. [2]Department of Chemistry, School of Sciences and Humanities, Nazarbayev University, 010000 Astana, Kazakhstan. [3]School of Chemical Engineering, Kazakh-British Technical University, 050000 Almaty, Kazakhstan. [4]Present Address: Lab of Renewable Energy, National Laboratory Astana, Nazarbayev University, 010000 Astana, Kazakhstan.

Discover Nano (2025) 20:68 | https://doi.org/10.1186/s11671-025-04231-9

In recent years, the demand for rapid and accurate gas sensors has grown significantly, as evidenced shown in Fig. 1 by the increasing number of publications on polymer gas sensors from 2013 to 2023 (Web of Science). PANI's intrinsic properties—ease of synthesis, room-temperature stability, and sensitivity to surface charges—have driven efforts to enhance its performance by forming hybrid composites with materials like metal oxides (e.g., $V_2O_5$, $TiO_2$, ZnO) [21–24]. These heterojunction structures improve gas sensing performance by providing effective charge transfer and enhanced active sites for gas adsorption [25, 26].

Recent advancements in PANI-based hydrogen sensors have centered on developing nanostructured materials to enhance sensitivity and selectivity. The current focus involves leveraging PANI nanofibers in various sensor configurations [27, 28]. These nanofibers exhibit high performance in hydrogen detection due to their well-ordered structure and significant surface-to-volume ratio, which facilitates efficient gas diffusion and adsorption [11, 29].

Studies have shown that highly ordered PANI nanofibers, particularly those deposited on gold or platinum electrodes, operate effectively as resistive hydrogen sensors [30–32]. Additionally, researchers have explored PANI-based gas sensors for detecting other gases, such as hydrogen sulfide, using advanced fabrication techniques like piezoelectric inkjet and screen printing [33–36]. Notably, hybrid composites of PANI with graphene or palladium nanoparticles demonstrate enhanced functionality, enabling the simultaneous detection of hydrogen and moisture [31, 37–39].

This review article represents the first specific review dedicated exclusively to PANI-based hydrogen sensors. It bridges gaps in understanding how different materials interact with PANI to optimize hydrogen sensing properties. Unlike other works that focus on limited synthesis techniques, this article compares multiple methods, offering a broader perspective for researchers interested in material properties,providing a roadmap for optimizing PANI-based materials for sensor applications.

### 1.1 PANI sensors' mechanism

As a conductive polymer, PANI has different structures in different doping states, and this structural change will lead to changes in the conductive properties, as shown schematically in Fig. 2, which shows the transition. PANI can undergo reversible doping under acidic or basic conditions. In acidic environments, protonation of the imine nitrogen induces charge carriers, increasing conductivity ($\sigma > 1$ S $cm^{-1}$) in the doped state (emeraldine salt), while the un-doped state (emeraldine base) exhibits very low conductivity ($\sigma < 1 \times 10^{-1}$ S $cm^{-1}$) [21, 41].

PANI's strong propensity to form hydrogen bonds allows for self-assemble layer by layer manner [42]. This self-assembly process can be enhanced by interactions with water-soluble compounds such as polyethers, polyalcohols, and cyclic polyamides [43].

Figure 3 illustrates a possible mechanism of hydride formation between PANI and hydrogen. The process of hydride formation between PANI and hydrogen involves several key steps. Upon exposure to hydrogen, the hydrogen molecules interact with the amine nitrogen along the PANI backbone, leading to $H_2$ dissociation [24, 28, 29]. This interaction results in the formation of N–H bonds between neighboring PANI chains, creating a polaron lattice [44, 45]. The charge transfer

**Fig. 1** Number of publications on gas sensors based on polymer materials by the past decade. The data were collected using the web of science—web of science core collection search: keywords of "polyaniline" AND "chemical sensor" OR "gas sensor" were used

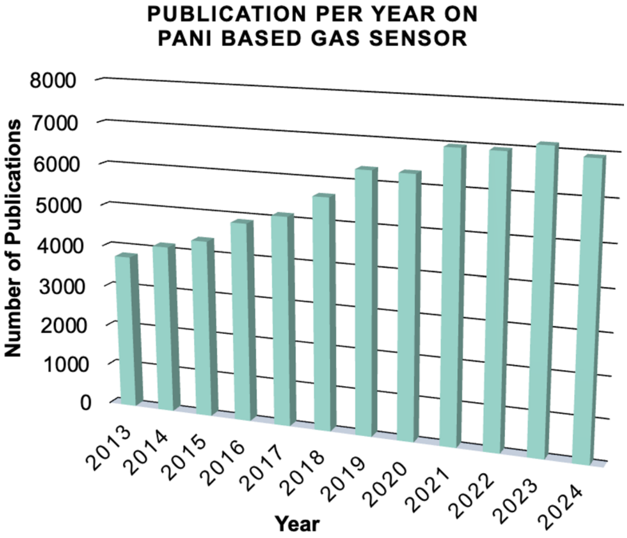

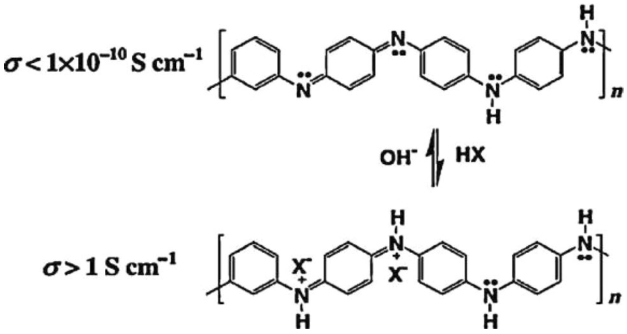

**Fig. 2** Repeating unit of polyaniline in its emeraldine oxidation state: on the top—undoped base form, and on the bottom—fully doped, acid form. Source: Reproduced with permission from Ref [40]. Copyright © 2020, Asian Association for Atmospheric Environment

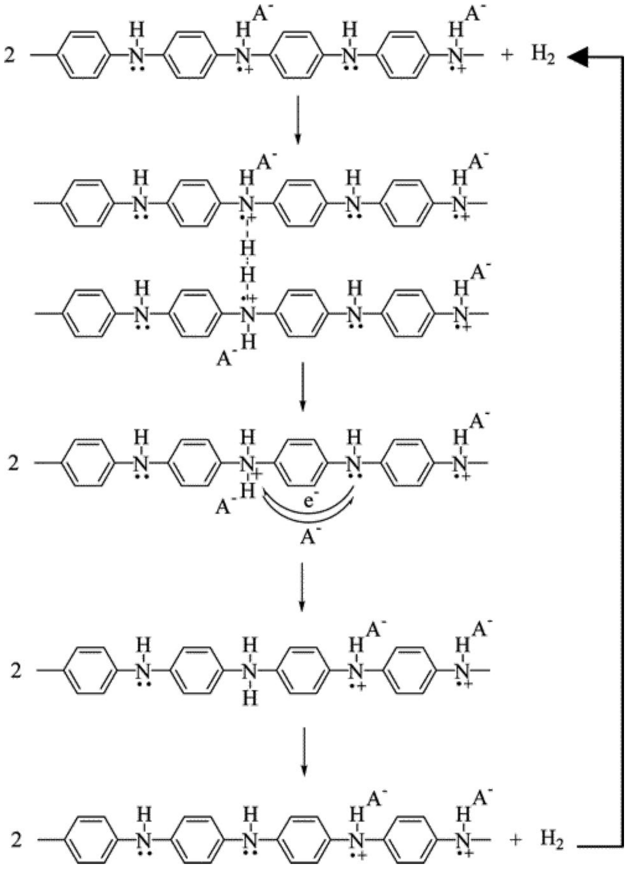

**Fig. 3** Possible mechanism for interaction between hydrogen and PANI. Source: Reproduced with permission from Ref. [28] Copyright © 2006, American Chemical Society

between these neighboring chains occurs as a result of this new formation, which will redistribute the polaron lattice density increasing the charge carrier concentrations [28, 46].

## 1.2 Nanostructure influence

In sensor applications, surface area is a critical parameter to consider, as it directly impacts the sensor's adsorption and response capabilities. PANI, as a CP, can be synthesized using various methods to achieve diverse nanostructures [47, 48]. Some of these nanostructures exhibit high surface areas, which provide abundant adsorption sites for gas molecules, facilitating rapid interactions and responses [49, 50]. Consequently, in PANI-based composites, the nanostructure of the material plays a pivotal role in determining its sensing performance.

Nanostructures such as nanofibers, nanowires, and nanotubes offer significantly higher surface-to-volume ratios compared to bulk materials [50]. This feature improves molecule diffusion and results in robust sensor responses due

**Table 1** Comparison of sensing performance in different PANI based hydrogen gas sensors

| Sensing materials | $H_2$ gas concentration | Sensitivity(%) | Response time(s) | References |
|---|---|---|---|---|
| PANI/$TiO_2$ | 2500 ppm | 9.05 | 94 | [23] |
| PANI/$Sm_2O_3$ | 10,000–80,000 ppm | 3.94 | 7 | [25] |
| MWNT/PANI | 500 ppm | 2.1 | 150 | [58] |
| MWCNTs/PANI | 0.4 vol% | 25 | 100 | [59] |
| PANI hollow nanotubes | 1–100 ppm | 29 | 15 | [12] |
| PANI thin film | 1–100 ppm | 20 | 65 | [12] |
| PANI nanofiber | 1–100 ppm | 6 | 102 | [12] |

**Table 2** Comparison of different nanostructure PANI materials' surface area

| Synthesis method | Nanostructure | BET Surface area($m^2/g$) | References |
|---|---|---|---|
| Template | PANI nanotubes | 77.1 | [60] |
| | PANI nanospheres | 67.9 | [60] |
| | PANI nanofibers | 30.9 | [60] |
| Interfacial polymerization | PANI hollow nanotubes | 35.2 | [61] |
| | PANI nanofibers | 28.1 | [61] |
| | PANI nanospheres | 13.9 | [61] |
| | PANI nanofibers | 37–54.6 | [62] |
| In situ polymerization | PANI nanoparticles | 53.1 | [63] |
| Hydrogel | PANI hydrogel | 41.6 | [64] |

to the increased number of active adsorption sites [51]. Furthermore, the reduction of materials to nanoscale dimensions often introduces novel properties, further enhancing the sensing characteristics of PANI-based composites [50]. For instance, Table 1 presents the performance of various PANI-based hydrogen sensors, highlighting the influence of different nanostructures on sensitivity and response times. Hollow nanotubes exhibit the highest sensitivity (29%) and a short response time (15 s) at low hydrogen concentrations (1–100 ppm), emphasizing the superior adsorption and diffusion properties of their morphology [12].

Tailoring PANI's nanostructure through methods such as interfacial polymerization, self-assembly, and electrospinning allows optimization of its gas-sensing performance [40, 52, 53]. Nanostructuralization using reactive ion etching, for example, has been shown to increase the sensitive surface area and introduce functional groups, significantly enhancing ammonia sensing performance [54]. One-dimensional (1D) nanostructures, such as nanotubes and nanofibers, are particularly advantageous due to their high surface-to-volume ratios and tunable electrical properties. The hollow, uniform structures of PANI nanotubes provide rich ion pathways and facilitate fast diffusion, improving both electrochemical and sensing responses [55].

The synthesis method also plays a crucial role in determining the surface area and morphology of PANI nanostructures. Table 2 illustrates how different synthesis techniques influence the specific surface area of PANI nanostructures, as measured by Brunauer–Emmett–Teller (BET) analysis. For example, PANI nanotubes synthesized using a template method achieve a surface area of 77.1 $m^2/g$, significantly higher than PANI nanofibers synthesized through interfacial polymerization (28.1 $m^2/g$). These variations in surface area directly impact sensing performance, as materials with higher surface areas provide more active sites for gas adsorption. Virji et al. [28] investigated the differences in hydrogen gas sensing performance between commercial PANI films and PANI nanofibers (as shown in Fig. 4). Their study demonstrates that hydrogen sensors based on nanostructured PANI are significantly more sensitive than those using commercial PANI films.

Incorporating PANI with other nanomaterials further influence morphology and enhances its gas-sensing capabilities. For instance, Pd-PANI-rGO nanocomposites demonstrate high sensitivity and selectivity to hydrogen gas at room temperature [56], with performance attributed to the spillover effect from palladium, efficient hydrogen dissociation, and the high surface area of the PANI-graphene oxide composite [56]. Similarly, electrospun PANI nanofibers are particularly effective due to their superior surface area and efficient charge/ion transport [57].

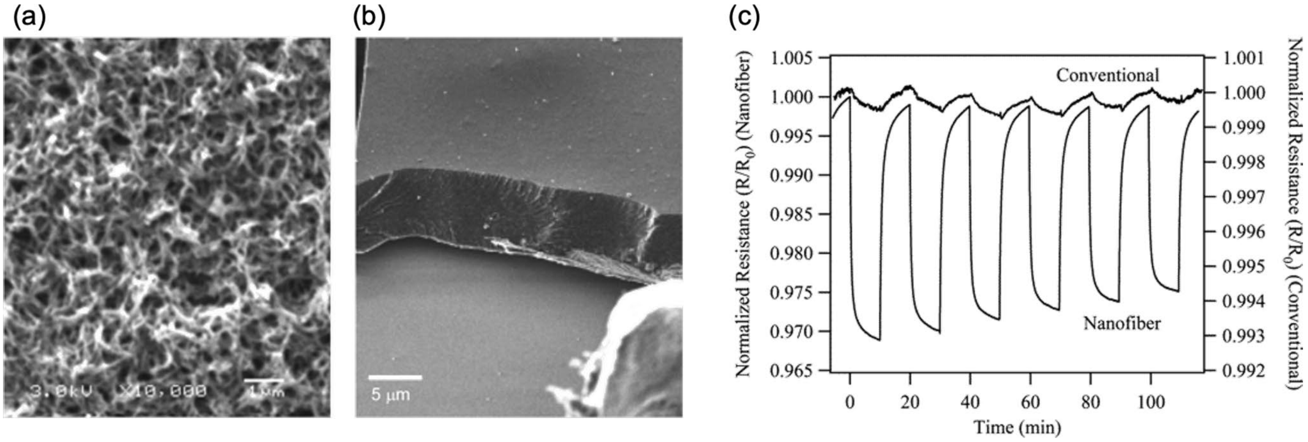

**Fig. 4** **a** SEM images of synthesis PANI nanofibers, **b** commercial PANI film, **c** response of commercial PANI film and PANI nanofiber films exposed to 1% $H_2$ gas. Source: Reproduced with permission from Ref [28]. Copyright © 2006, American Chemical Society

All these findings demonstrate that the nanostructure of PANI plays a crucial role in its sensing performance by offering a high specific surface area, facilitating improved molecular diffusion, and enhancing adsorption capabilities. Advances in synthesis techniques allow precise control over PANI's morphology, enabling the development of high-performance gas sensors.

## 2 PANI-based hybrid materials for advanced sensors

The enhancement of sensing properties in PANI-based sensors through the incorporation of additional materials, such as metal oxides or carbon-based nanomaterials, has been a focal point of recent research. PANI's intrinsic properties, including high conductivity, tunable morphology, and environmental stability, can be significantly improved when combined with these nanomaterials. The resulting hybrid materials exhibit enhanced sensitivity, faster response times, and improved selectivity in gas sensing applications.

This improvement arises from the synergistic effects between PANI and the incorporated nanomaterials. These effects include enhanced charge transfer kinetics, increased surface area for gas adsorption, and modified electronic properties of the sensing material, as shown in Table 3. Various studies have demonstrated the superior performance of PANI-based hybrid materials in detecting gases such as ammonia, hydrogen, and volatile organic compounds (VOCs) [5–7, 11]. Table 4 provides a comparative overview of the approximate costs per gram for various materials commonly used in sensing applications. It underscores the significant cost differences among these materials, which play a critical role in material selection, particularly when considering budget constraints and specific application requirements. These cost variations are essential for assessing the feasibility of large-scale production and implementation, as they directly influence the overall cost of developing sensing technologies.

Sections 2.1 and 2.2 provide a detailed discussion of:

2.1 PANI with carbon-based nanomaterial composites;
2.2 PANI with metal oxide nanomaterial composites.

**Table 3** Performance enhancement of PANI-based gas sensors with various nanomaterials

| Property | Nanomaterial | References |
|---|---|---|
| Enhanced conductivity and sensitivity | Graphene, carbon nanotubes, metal and metal oxides (e.g., ZnO, $TiO_2$) | [23, 29, 65–67] |
| Increased surface area | Nanostructured materials, including graphene and hybrid composites | [65, 68–73] |
| Synergistic effects | n-type nanomaterials such as graphene, metal oxides | [67, 74, 75] |
| Improved stability and selectivity | Metal oxides, graphene, other functional nanomaterials | [76, 77] |
| Flexibility and processability | Flexible substrates combined with nanomaterials such as graphene and other composites | [69, 78] |

**Table 4** Comparative table summarizing the approximate costs per gram for the specified materials

| Material | Approximate cost (per gram) |
|---|---|
| Polyaniline (PANI) | \$1–\$5 |
| Polypyrrole (PPY) | \$1–\$5 |
| Polythiophene (PTh) | \$5–\$10 |
| PEDOT | \$10–\$20 |
| Single-walled carbon nanotubes (SWCNT) | \$100–\$500 |
| Multi-walled carbon nanotubes (MWCNT) | \$50–\$100 |
| Graphene | \$50–\$100 |
| Titanium dioxide ($TiO_2$) | \$0.10–\$0.50 |
| Tantalum | \$2–\$5 |
| Samarium oxide ($Sm_2O_3$) | \$10–\$20 |
| Tin oxide ($SnO_2$) | \$0.50–\$1 |
| Palladium oxide (PdO) | \$50–\$100 |
| Zinc oxide (ZnO) | \$0.10–\$0.50 |

These sections highlight the improvements, mechanisms, and synthesis approaches for these hybrid materials.

## 2.1 Nanocarbons/PANI materials

Nanocarbon/PANI composites represent a significant advancement in hydrogen sensing technologies due to their enhanced conductivity, selectivity, and sensitivity. These materials leverage the unique properties of conducting polymers and carbon nanostructures, such as carbon nanotubes (CNTs) and graphene [59, 74], to improve sensor performance. The integration of nanocarbons into PANI matrices results in composites that exhibit increased surface area and improved electron transfer capabilities, which are critical for effective gas sensing. These composites respond to hydrogen gas through changes in electrical resistance, which is facilitated by the adsorption of hydrogen molecules on the nanocarbons and their subsequent interaction with the PANI matrix [56, 58]. Studies have shown that incorporating multi-walled carbon nanotubes (MWCNTs) [58] and reduced graphene oxide (rGO) [56] into PANI not only enhances the material's conductivity but also significantly boosts its sensitivity and response time to hydrogen gas at room temperature. These advances make nanocarbon/PANI composites highly promising for developing high-performance, room-temperature hydrogen sensors.

### 2.1.1 Sensing performance

**2.1.1.1 SWCNT/PANI** Shrivastava et al. [58] synthesized PANI through the chemical oxidative polymerization of aniline, and used ultrasonication to mix PANI with SWCNT to form target material. The sensing performance of SWCNT/PANI and MWCNT/PANI composites, as shown in Fig. 5, highlights that these hybrids demonstrate significant improvements in gas detection capabilities. The integration of SWCNTs with PANI enhances the composite's sensitivity and response time due to the high surface area and excellent electrical properties of SWCNTs. This results in a more effective interaction between the gas molecules and the sensing material. Similarly, the use of MWCNTs in the PANI matrix also contributes to improved sensing performance. The MWCNT/PANI composites exhibit a robust sensing response attributed to the multiple conductive pathways provided by the MWCNTs, which facilitate efficient charge transfer and gas adsorption. Both SWCNT/PANI and MWCNT/PANI composites demonstrate superior sensitivity, selectivity, and rapid response times in gas sensing applications compared to pure PANI, making them highly suitable for advanced gas sensor technologies [58].

**2.1.1.2 MWCNT/PANI** Bafandeh et al. [79] synthesized MWCNT/PANI composites via chemical oxidative polymerization with acid sulfonic camphor (CSA) as a strong acid for protonation of EB PANI, incorporating MWCNTs at concentrations of 1, 2, and 4 wt% (Fig. 6). The MWCNTs were individually dispersed in 5 ml of chloroform through ultrasonication for 2 h, followed by their integration into pure PANI using ultrasonication, resulting in samples designated as P1(PANI + 1 wt%of MWCNT), P2(PANI + 2 wt% of MWCNT), and P3(PANI + 4 wt% of MWCNT).

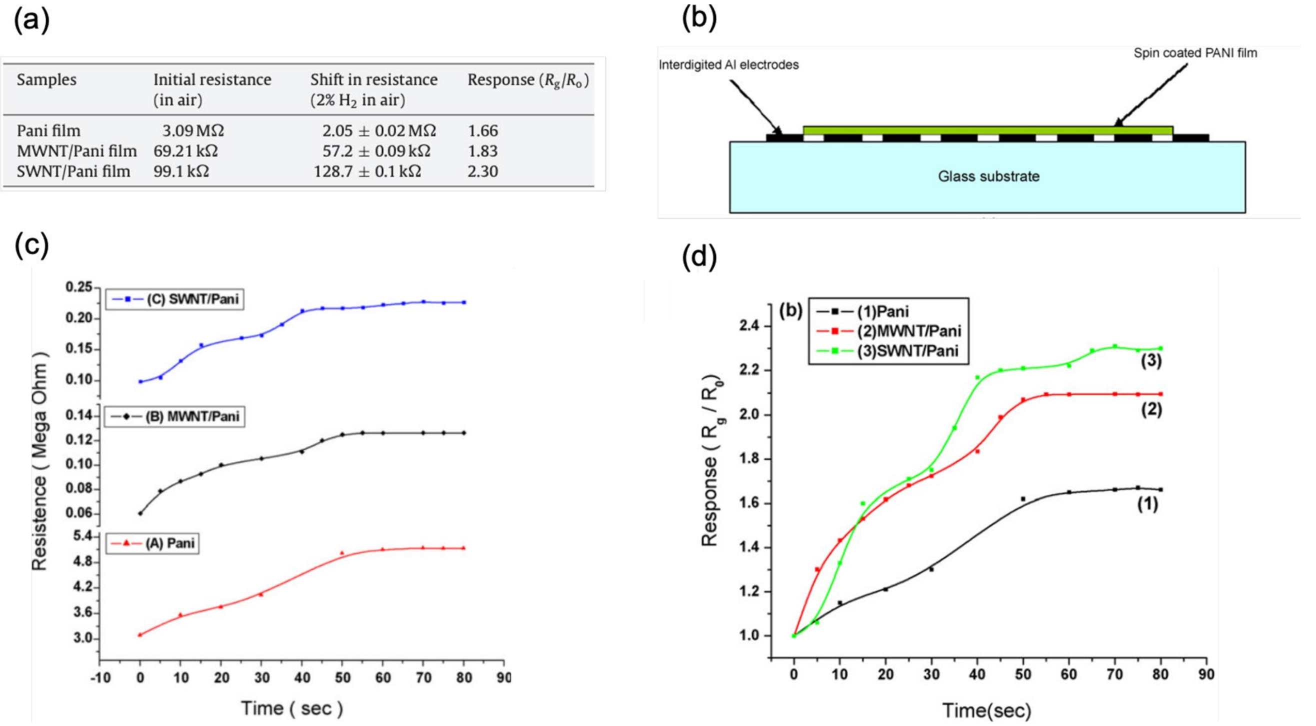

(a)

| Samples | Initial resistance (in air) | Shift in resistance (2% $H_2$ in air) | Response ($R_g/R_o$) |
|---|---|---|---|
| Pani film | 3.09 MΩ | 2.05 ± 0.02 MΩ | 1.66 |
| MWNT/Pani film | 69.21 kΩ | 57.2 ± 0.09 kΩ | 1.83 |
| SWNT/Pani film | 99.1 kΩ | 128.7 ± 0.1 kΩ | 2.30 |

**Fig. 5** **a** The comparison of response and resistance in PANI samples before and after exposure to 2% hydrogen gas; **b**Schematic diagram of sensing electrode; **c** Resistance changes of composite in 2% $H_2$; **d** Response of composite in 2% $H_2$. Source: Reproduced with permission from Ref [58]. Copyright © 2009 Elsevier B.V. All rights reserved

Figure 6 illustrates the significant enhancements in gas detection capabilities of these composites. The incorporation of MWCNTs into the PANI matrix leads to a composite with improved sensitivity and response for 0.4 vol% hydrogen gas sensing. The high surface area and excellent electrical conductivity of MWCNTs facilitate efficient charge transfer and gas molecule adsorption, resulting in a more effective sensing response. Additionally, the multiple conductive pathways provided by MWCNTs enhance the overall conductivity of the composite, further boosting its sensing performance. Compared to pure PANI, the MWCNT/PANI composite exhibits superior performance in detecting gases [79].

These findings align with other studies that have demonstrated the enhanced gas sensing properties of MWCNT/PANI composites. For instance, research [59] has shown that increasing the CNT content in CNT/PANI composites improves electrical properties and reduces the optical bandgap, contributing to better sensing performance. Furthermore, Bafandeh et al. [79] demonstrated that MWCNT/PANI nanocomposite films maintain good stability over a three-month period, indicating their potential for long-term gas sensing applications. Hence, the integration of MWCNTs into the PANI matrix significantly enhances the composite's gas sensing capabilities, making it a promising material for detecting various gases with high sensitivity and selectivity.

### 2.1.2 Sensing performance based on graphene/PANI

Graphene is a promising material for enhancing the sensing performance of PANI. Its high surface area, planar structure, superior conductivity, and synergistic interactions with PANI contribute to more effective sensor integration. Unlike the synthesis processes for SWCNT/PANI and MWCNT/PANI composites, Al-Mashat et al. [29] developed a graphene/PANI nanocomposite by mixing aniline and graphene prior to polymerization, followed by ultrasonication to achieve uniformity.

The resulting nanocomposite (Fig. 7) exhibited a significant enhancement in sensitivity compared to its individual components, attributed to the synergistic interaction between graphene's high surface area and electrical properties and PANI's responsive characteristics. Specifically, the graphene/PANI nanocomposite-based sensor demonstrated a sensitivity of 16.57% towards a 1% hydrogen gas concentration (Fig. 7a), outperforming sensors made solely from graphene or PANI nanofibers. This improved performance is primarily due to the effective integration of graphene,

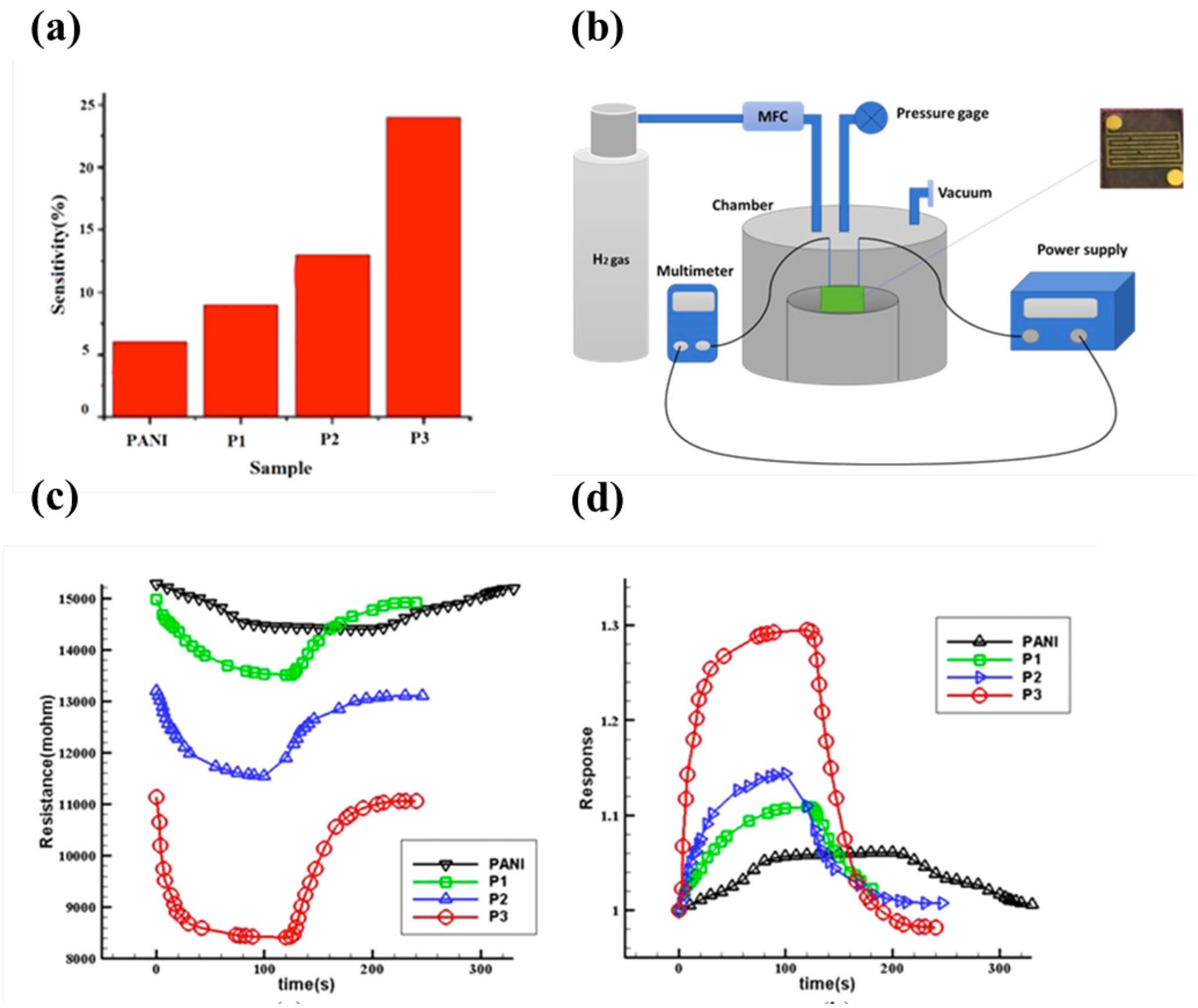

**Fig. 6** **a**sensitivity of different samples: pure PANI, P1: PANI + 1% of MWCNT, P2:PANI + 2% of MWCNT, P3: PANI + 4% of MWCNT; **b** Schematic diagram of gas sensing setup; **c** Resistance changes of PANI films in 0.4 vol.% $H_2$. **d** Corresponding dynamic responses recovery of PANI thin filmsin 0.4 vol.% $H_2$. Source: Reproduced with permission from Ref [79]. Copyright © 2023, Bafandeh, Nastaran; Solaymani, Shahram. This article is distributed under a Creative Commons Attribution (CC BY) license

which provides a conductive network that supports the dispersion and stabilization of PANI, thereby enhancing interactions with hydrogen molecules.

The XPS spectrum of the graphene/PANI nanocomposite (Fig. 7b) reveals detailed information about the carbon (C) and nitrogen (N) environments, which are critical due to their role in the electronic and structural characteristics of the composite. The C1s spectrum typically shows peaks that can be attributed to different carbon states related to both graphene and PANI. For instance, you might see a peak at around 284.6 eV corresponding to C–C bonds (indicative of graphene), and other peaks that suggest the presence of C-N bonds, which are characteristic of PANI. This differentiation helps confirm the successful integration of PANI onto the graphene sheets.

In practical applications, graphene/PANI sensors utilize a conductometric sensing mechanism, measuring changes in resistance upon exposure to hydrogen gas. This configuration benefits from the nanocomposite's morphology, where PANI uniformly covered the graphene sheets, forming a consistent structure that increases the active surface area available for gas interactions (as shown in Table 5), and facilitating efficient charge transfer between PANI and graphene. This synergistic effect leads to improved sensing performance in gas detection.

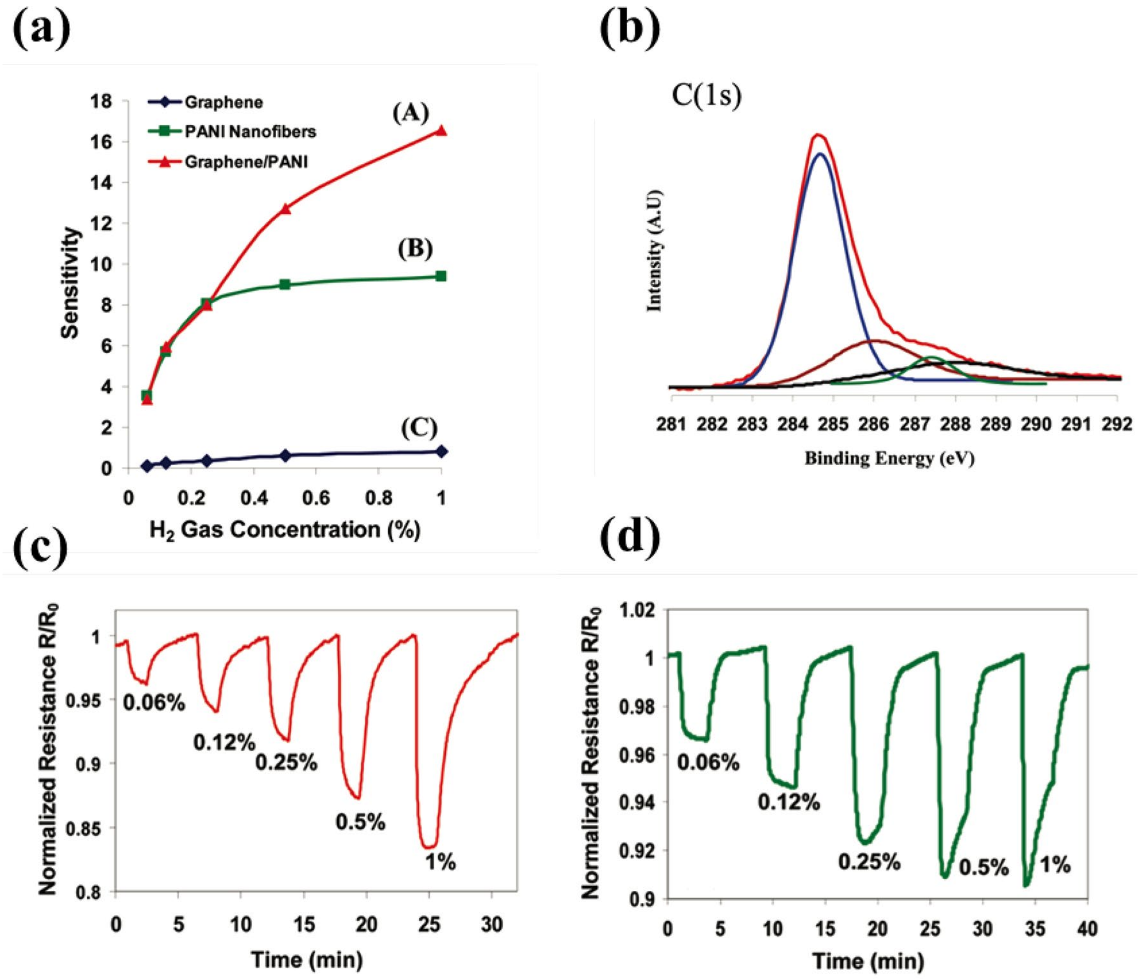

**Fig. 7** **a**The sensitivity of different samples: graphene/PANI, PANI nanofibers, Graphene; **b** XPS peak for the graphene/PANI nanocomposite; **c** The sensing responses of the graphene/PANI; **d** The sensing responses of PANI nanofibers. Source: Reproduced with permission from Ref. [29] Copyright © 2010, American Chemical Society

**Table 5** BET surface area analyses of PANI and graphene/PANI [80]

| Samples | BET surface area ($m^2/g$) | Pore volume ($cm^3/g$) | Pore diameter (nm) |
|---|---|---|---|
| PANI | 38.6154 | 0.139096 | 13.39647 |
| Graphene/PANI | 41.5321 | 0.194556 | 20.15315 |

## 2.2 Metal oxide/PANI materials

### 2.2.1 PANI-metal oxides hybrid nanocomposite for hydrogen gas sensors

In the field of hydrogen gas detection, researchers have focused on utilizing PANI and metal oxides to develop sensitive and selective gas sensors. Various studies have been conducted to enhance the detection capabilities of these materials specifically for hydrogen gas [81–83].

Metal oxides, including ZnO, $SnO_2$, $TiO_2$, and $WO_2$, have been used extensively in the field of gas sensors due to their remarkable chemical stability, large surface areas, and active surface sites that are capable of adsorbing gases effectively [23, 24, 84, 85]. However, because of their limited selectivity and high working temperatures, they frequently experience problems. Combining PANI with metal oxides leverages the distinct advantages of both materials, resulting in enhanced gas sensing capabilities. This synergy leads to improved sensitivity, enhanced selectivity, and reduced operating temperatures [85].

### 2.2.2 Preparation methods of PANI-metal oxide hybrid nanocomposites

Several techniques for synthesizing composites of PANI and metal oxides are available:

The sol–gel method is employed to synthesize metal oxides, which are subsequently combined with PANI using electrochemical deposition. This methodology enables precise control over the composite structure. Mashao et al. [86] synthesized PANI by polymerizing aniline using ammonium persulfate (APS) as the oxidizing agent. They then prepared a zinc-based zeolitic benzimidazolate framework (ZnZIF) by reacting zinc chloride with benzimidazole. The PANI-ZnZIF composite was then created through in-situ oxidative polymerization of aniline in the presence of ZnZIF, resulting in a nanocomposite material.

Srivastava et al. [87] synthesized a $TiO_2$/PANI composite by conducting in-situ chemical oxidative polymerization of aniline in the presence of colloidal $TiO_2$ nanoparticles, using APS as the oxidant. The preparation method described by Nasirian et al. [88]involves synthesizing $TiO_2$ nanoparticles by adding titanium tetrachloride, followed by gel formation and calcination to obtain anatase or rutile-phase $TiO_2$ nanocomposites. In the sol–gel technique, hydrolysis and condensation are critical processes for achieving the desired characteristics of metal oxides. Pure PANI and PANI/$TiO_2$ nanocomposites (PTeNCs) were synthesized using in-situ chemical oxidative polymerization of aniline with APS as the oxidant.

Moghaddam et al. [89] synthesized a PANI/titania nanocomposite by dispersing titania nanoparticles into an aniline solution. APS solution was then added dropwise at a low temperature. The titania content was varied by adjusting the quantity of titania in the aniline solution prior to polymerization. The resulting nanocomposite was doped with 10-camphor sulfonic acid and applied onto epoxy glass substrates with Cu-interdigitated electrodes via spin-coating to create sensors.

Srivastava et al. [90] synthesized PANI using in-situ oxidative polymerization, where aniline is chemically oxidized to form PANI. They then applied a spin-casting technique to deposit thin layers of PANI onto finger-type copper (Cu) interdigitated electrodes, enhancing the sensor's surface area for gas interaction. A thin layer of tantalum (Ta) was subsequently coated onto the PANI films to create Ta/PANI composite chemiresistor sensors, combining the conductive properties of PANI with the reactivity of Ta for improved hydrogen gas sensing. The composite films were later exposed to high-energy $Au^{+12}$ ion irradiation at varying fluences, allowing the researchers to investigate how different levels of ion exposure affect the films' structural and electrical properties, ultimately influencing their gas sensing performance. Similarly, the PANI/$Sm_2O_3$ nanocomposite was synthesized using an in-situ chemical oxidation polymerization technique [25]. $Sm_2O_3$ microspheres were dispersed in an aniline solution at a low temperature, and APS solution was gradually added to form a dark green PANI/$Sm_2O_3$ nanocomposite.

Incorporating Pd into composite systems significantly enhances functionality. For instance, Pd plays a crucial role in PANI/$SnO_2$/Pd nanocomposite films, particularly for hydrogen sensing applications [84]. Palladium nanoparticles act as catalysts for hydrogen molecule dissociation into hydrogen atoms, forming PdHx. The Pd nanoparticles facilitate electron transfer with $SnO_2$, while hydrogen atoms within the Pd lattice scatter electrons. Furthermore, PdO nanoparticles have been utilized to improve the sensing properties of PANI-based nanocomposites for hydrogen detection [91]. Adding PdO nanoparticles to the PANI matrix increases electron density and barrier width, improving sensitivity and response to hydrogen gas at ambient temperature. The preparation process involved oxidative polymerization of aniline in a solution containing PdO nanoparticles and APS as the oxidizing agent. The nanocomposite powders obtained are transformed into a conductive state through doping with CSA, which facilitates the conversion of PANI to its conductive emeraldine salt form, significantly enhancing its conductivity. And the resulting powder is deposited as thin films on ITO-coated glass substrates. These films served as hydrogen sensing elements, eliminating the need for expensive interdigitated electrodes.

## 2.3 Gas sensing principle of hybrid conducting polymer-metal oxide nanocomposites

Hybrid nanocomposites consisting of conducting polymers and metal oxides have become highly useful materials for gas sensing applications, thanks to their exceptional combination of characteristics. To fully understand the gas-sensing concept of these hybrid materials, one must examine the interactions between the molecules of gas and the composite material and also the subsequent changes in the material's electrical properties.

PANI-based metal oxide composites, specifically PANI/ZnO composites, have demonstrated potential in gas sensing applications, particularly in the detection of hydrogen gas [83]. The simulations demonstrate a significant enhancement in the sensitivity of $SnO_2$ to $H_2$ gas molecules after combining it with Pd. Similarly, the sensitivity of PANI to $H_2$ gas molecules is considerably improved after combining it with $SnO_2$. Among all the films, the $SnO_2$/Pd film exhibits the highest sensitivity at room temperature, reaching approximately 540% for a gas concentration of 0.4%. In addition, Ag–$SnO_2$ nanofibers were produced using the electrospinning approach. The 2% Ag–$SnO_2$ composite exhibited superior stability, minimal response time, and rapid recovery time in comparison to both pure $SnO_2$ and other composites across all hydrogen gas concentrations. The sensing mechanism of Ag-doped $SnO_2$/PANI nanofibers can be explained by the formation of a depletion layer between the p-type PANI and the n-type Ag–$SnO_2$ [52, 92]. Furthermore, nanofibers consisting of PANI and aluminium doped tin oxide (Al–$SnO_2$/PANI) have been produced using the electrospinning approach for the purpose of sensing hydrogen gas. When exposed to hydrogen gas at a concentration of 1000 ppm, the nanofibers of the Al–$SnO_2$/PANI composite showed a high level of sensitivity at 48 °C. Additionally, the response and recovery times of the composite nanofibers were faster compared to those of pure $SnO_2$ [93].

A study was conducted to investigate the gas sensing capabilities of $TiO_2$ nanotube arrays. $TiO_2$ nanostructures are considered ideal functional materials for hydrogen gas sensing due to their exceptional chemical stability, large surface area, non-toxicity, and compatibility with various sensing methods. Among the many semiconductor metal oxides, $TiO_2$ nanostructures have proven to be particularly efficient. The study revealed that $TiO_2$ nanotube arrays exhibit a significant response and suitable selectivity toward $H_2$ gas at an operating temperature of 300 °C [94]. PANI can enhance the transfer of electric charge between the gas molecules and other constituents of the composite material. The hydrogen gas detecting mechanism of the porous PANI tube-like/$TiO_2$ nano-heterostructure (PPTH) is based on the chemisorption of $H_2$ gas molecules onto the material's surface, resulting in alterations in the sensor's electrical conductivity. The interaction between $H_2$ and the PPTH structure leads to alterations in the concentration and mobility of charge carriers inside the material, resulting in a detectable change in resistance [23]. This change in resistance acts as a signal for the presence of hydrogen gas, with higher sensitivity showing the sensor's capacity to detect low amounts of hydrogen. Nasirian et al. [88]. conducted research on the influence of various titania phases on the hydrogen gas sensing properties of PANI/$TiO_2$ nanocomposite. The study determines that the distinct stages of titania (anatase and rutile) have a substantial impact on the ability of PANI/$TiO_2$ nanocomposites to detect hydrogen gas. Rutile $TiO_2$ has stronger thermal stability and a lower band gap than other phases, allowing for increased charge carrier mobility and interaction with hydrogen molecules. The addition of rutile in the nanocomposite improves its specific surface area and porosity, resulting in more active sites for gas adsorption and reaction. It was found that sensors with 40 wt% rutile $TiO_2$ nanoparticles exhibited a reproducible response to 0.8 vol% hydrogen gas at room temperature [87, 89]. On the other hand, the inclusion of anatase $TiO_2$ nanoparticles into the PANI matrix might promote the development of an n-p heterojunction, hence improving charge carrier transport and electron transfer between the two materials. When exposed to hydrogen gas, this interaction reduces resistance while increasing conductivity because the $TiO_2$ nanoparticles provide alternative paths for electron transport. Furthermore, the well-dispersed anatase nanoparticles increase the surface area for gas adsorption, which improves interaction with hydrogen molecules [95]. Additionally, the increase in resistance is likely caused by the improved alignment (better packing) of anatase $TiO_2$ nanoparticles as well as PANI matrix compared to rutile nanoparticles and PANI matrix.

Farooqi et. al. developed a composite material known as PANI Zinc Oxide (PANI-ZnO), which results in a substantial enhancement in the interaction energy between the composite sensor and hydrogen molecules. The investigation revealed that the composite sensor exhibited a binding affinity of around 42.8 kcal/mol with hydrogen gas, indicating a robust interaction energy [83]. The heightened interaction between components causes alterations in the electrical configuration and conductive properties of the substance, leading to heightened sensitivity to hydrogen gas. In addition, the composite sensor exhibited nearly double the level of interaction energy with hydrogen in comparison to other substances, including ethanol, methanol, and acetone. The results emphasize the efficacy of the PANI-ZnO composite sensor in detecting hydrogen gas, indicating its potential as a material for hydrogen sensing in the monitoring and treatment of industrial effluents.

Palladium (Pd) and palladium-based alloys have been extensively studied as $H_2$ sensors because of their rapid reaction and exceptional sensitivity to $H_2$ gas, even at ambient temperatures [96, 97]. In addition, Pd was employed for the decoration of the polymer. The preparation process entails the synthesis of Pd-decorated nanoporous poly(aniline-co-aniline-2-sulfonic acid):poly(4-styrenesulfonic acid)(PANI-co-ASA):PSS) nanostructures[98]. Palladium(II) chloride is used as a catalyst to detect hydrogen by generating compounds with sulfonic acid groups (Fig. 8). Also, ammonium bicarbonate is used to stimulate the creation of pores when heated, so increasing the surface area facilitates better hydrogen transport.

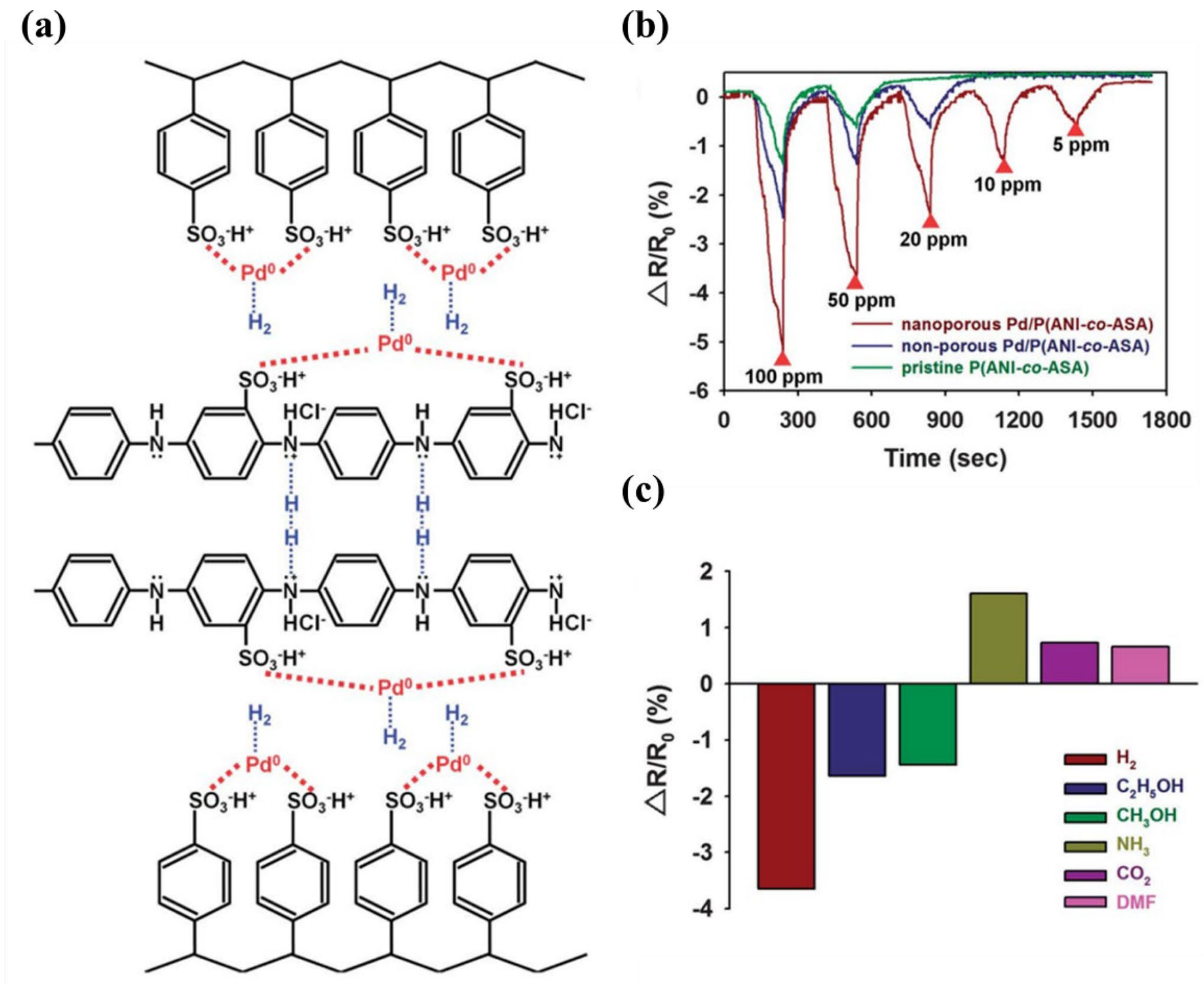

**Fig. 8** **a** Potential mechanisms for molecular interactions between Pd-decorated copolymer and $H_2$ gas molecules, **b** Dynamic responses of copolymer to $H_2$ (5 to 100 ppm), **c** response of copolymer to different gases. Source: Reproduced with permission from Ref [98]. Copyright © 2013, Royal Society of Chemistry

The Pd-decorated P(ANI-co-ASA):PSS nanostructure interacts with $H_2$ gas molecules by two primary methods: hydrogen bonding with amine nitrogen positions along the polymer backbone and absorption by neutral Pd nanoparticles connected to the nanostructure. These interactions have the effect of facilitating charge transfer and resistivity changes, which in turn increases the sensitivity of the nanostructures to the detection of $H_2$ gas (Fig. 8a). The presence of nanoporous structures resulted in enhanced electron transport when exposed to $H_2$ gas, as a result of the greater surface area available for interaction with $H_2$ molecules. As a result, the nanoporous device exhibited consistent baseline resistance across a broad range of $H_2$ concentrations, in contrast to the pristine and Pd-decorated non-porous samples (Fig. 8b). The sensors utilizing P(ANI-co-ASA):PSS nanostructures exhibited a response time of under 90 s, with the initial resistance returning to normal within around 40 s. The swift reaction and recuperation demonstrated the effectiveness of the nanostructures in detecting hydrogen gas.

Heterostructure materials have attracted researchers' attention for gas sensing applications because of their distinctive chemical and electrical properties, which improve the sensitivity and response characteristics of the sensing device. Arora et.al [91] have created composites of PdO and PANI by a one-pot in-situ wet chemical assembly procedure. A thin coating of pure PANI, PANI with 5% PdO, and PANI nano-composites with 10% PdO are placed onto a glass substrate covered with an ITO layer using a sputtering process. The proposed heterostructure device exhibits significant sensitivity to hydrogen concentrations of 1%, 3%, 10%, and 20%.

To summarize, the study on PANI and metal oxides for hydrogen gas detection showcases notable progress in the creation of highly sensitive and specific gas sensors. The cited research showcase the potential of PANI-based materials in gas sensing technologies, namely for detecting hydrogen gas. This opens up possibilities for developing efficient and dependable gas sensors for a range of industrial and environmental monitoring purposes.

## 3 Challenges and prospects

The hydrogen sensors based on PANI have several advantages such as room-temperature operation and excellent electronic properties, easy fabrication, and low cost, compared to conventionally used metal oxide semiconductor (MOS) materials [84, 99]. However, PANI has several drawbacks compared to MOS, including (1) low hydrogen sensitivity, (2) poor thermal stability, and (3) limited solubility.

Pure PANI has poor sensitivity so it can't be used alone as a gas sensor[100]. In their work, Pippara et al. [84] reported that pure PANI films showed the least sensitivity when interacted with $H_2$ gas, compared to $SnO_2$ film, $SnO_2+Pd$ composite, and $SnO_2$/PANI nanocomposite. The gas sensing mechanism in PANI is due to the reduction of the imine (= N–) and amine (–NH–) groups with $H_2$ molecules. The resistance of the polymer film decreases with the protonation of the N atom. Whereas, in $SnO_2$/PANI nanocomposite $SnO_2$ is an n-type and PANI is a p-type material. Under the normal atmospheric condition oxygen gets absorbed on the $SnO_2$ surface by occupying oxygen vacancies that are formed during the hydrothermal synthesis. The adsorbed oxygen molecules capture the free electrons in the conduction band of n-type $SnO_2$, and form ($O^-$, $O^{2-}$) species. This leads to improvement in gas sensing property, as it increases the number of active sites for adsorption of gas molecules. In this gas sensing mechanism, $H_2$ molecules react with adsorbed oxygen species, and form free electrons alongside water molecules. These free electrons recombine with the holes which are major charge carrier species in p-type PANI. The overall charge neutralization reduces the number of charge carriers, and increases the resistance of the material.

It's prominent that gas adsorption is a key process in the sensing process alongside redox reactions. In their work, Kroutil et al. [101] tested different morphology of PANI layers for gas detection, and found that while adsorption is favored at room temperature, increasing temperature up to 80 ℃ shifts the equilibrium to the direction of gas desorption. In contrast, the sensing performance based on redox reactions tends to increase with higher temperature, due to increased reaction speed [99]. However, PANI is an organic compound, and can't withstand high temperatures at 200–500 ℃ as opposed to MOS. Therefore, low thermal stability is another limitation of PANI based sensors.

Another challenge faced by pure PANI gas sensors is poor solubility of CPs. PANI salt, emeraldine hydrochloride, is generally not soluble in common organic solvents. It was reported to be soluble only in concentrated sulfuric acid solution, and soluble in organic solvents such as chloroform, dimethylsulfoxide (DMSO), and xylene upon mixing with functionalized protonic acids such as CSA and dodecylbenzenesulfonic acid (DBSA) [102]. This factor limits PANI's compatibility with advanced fabrication techniques and restricts its ability to blend with functional additives. Many gas sensors rely on composite materials or coatings enhanced with nanoparticles or catalysts, but PANI's insolubility makes it challenging to achieve uniform mixtures or high-quality films. Additionally, this issue increases production complexity and costs, making it less feasible for large-scale manufacturing and commercial applications. Addressing solubility challenges is essential to improve PANI's adaptability and performance in sensor technologies.

### 3.1 Prospects

During the past decade, PANI manifested great potential for application in hydrogen gas sensing. Hybridization, or forming hybrid materials [103] of PANI with conventionally used metal oxide can improve the sensitivity of composite due to the synergistic effect, and overcome the limitations of pure PANI [100]. In their work, Pippara et al. [84] present a new type of $SnO_2$, PANI, and Pd hybrid films as promising ultra-high sensitive gas sensors. Pd doped PANI-$SiO_2$ films showed the highest ratio of sensitivity to total cycle time, which is the sum of response time and recovery time. The generation of more active sites for $H_2$ gas adsorption through the large precise surface area and microstructure of $SnO_2$ increases the sensing performance of hybrid composite. Additionally, Pd nanoparticles act as a catalyst by dissociating $H_2$ molecules into H atoms and PdH(x), for the adsorption of $H_2$ molecules onto the PANI-$SiO_2$ surface.

The conductivity of PANI like any other CP depends on the ability to transfer charge carriers along the polymer backbone, and for the carriers to hop between polymer chains. Thus, alteration of these processes directly affects the conductivity of PANI. For this reason, different nanostructured forms of PANI, including nanorods, nanowires, and nanofibers are of particular interest due to their increased surface area that allows faster diffusion of gas molecules into the gas sensor structure. For instance, Virji et al. [104] showed that thin films composed of PANI nanofibers exhibit faster response times and greater sensitivity than those produced by conventional methods. This improvement is attributed to more efficient charge transfer pathways and a higher density of active sites in the nanostructures. Moving forward, a promising prospect lies in the design of tailored nanostructures that optimize conductivity, mechanical stability, and diffusion efficiency. Further exploration of hybrid systems that combine PANI nanostructures with nanoparticles or two-dimensional materials like graphene could significantly enhance the performance of gas sensors. These advancements open the door to the development of ultra-sensitive, selective, and robust hydrogen gas sensors.

Overall, the high conductivity and unique doping mechanism, as well as room temperature sensing capability of PANI over conventionally used metal oxides, which require increased temperature to work, renders it to be a very promising material for hydrogen gas sensors. For this reason, PANI based sensors consume much less energy, and are superior for the development of low power sensors. Additionally, the flexibility of CPs, including PANI makes it a highly suitable material for integration into flexible devices over MOS. This property is especially practical for long-life sensor devices. Despite this, pure PANI based sensors still suffer from instability, weak sensing ability, and poor solubility. To overcome these limitations, significant work was put into hybridization of PANI with other inorganic materials, such as graphene, carbon nanotubes, metals, or metal oxides [99]. The synergistic effect of combining PANI with inorganic material leads to increased stability and sensing properties of composite, through reinforced adsorption and electronic interactions. Despite considerable research advancements, there are still concerns regarding gas selectivity, stability, and sensing response that hinder the practical application of PANI. Further efforts are required to resolve these issues and enhance PANI's suitability as sensors for real-world use.

## 4 Conclusion

This review highlights the significant advancements in the development of PANI-based hydrogen sensors, emphasizing the role of hybrid materials, nanostructured morphologies, and advanced synthesis techniques in enhancing their performance. The key findings of the study are summarized as follows:

### 4.1 Electrical properties

PANI and its hybrids demonstrate enhanced conductivity, particularly when combined with graphene, metal oxides, or carbon nanotubes. The composites exhibit significantly higher sensitivity and reduced resistance changes during hydrogen detection at room temperature.

### 4.2 Nanostructural influence

Morphological tailoring of PANI nanostructures (nanofibers, nanotubes, and nanospheres) significantly increases the surface area, as evidenced by BET analysis. PANI nanotubes achieved a surface area of 77.1 $m^2$/g, resulting in superior gas adsorption properties.

### 4.3 Sensing performance

Hybrid materials like PANI/ZnO and PANI/$SnO_2$ exhibit faster response and recovery times, with sensitivity reaching up to 29% at 15 s for PANI hollow nanotubes at 1–100 ppm hydrogen concentrations.

### 4.4 Synergistic effects in composites

Incorporation of palladium nanoparticles into PANI-based composites catalyzes hydrogen dissociation, enhancing the detection capabilities through a spillover mechanism.

### 4.5 Surface area and morphology

Graphene/PANI composites display improved gas adsorption due to synergistic effects and increased active surface areas, as confirmed by XPS analysis and pore diameter measurements (e.g., 20.15 nm for graphene/PANI vs. 13.4 nm for pure PANI).

Future research should address remaining challenges in stability, selectivity, and response time to fully exploit the potential of PANI-based sensors. Continued innovation in the synthesis and integration of PANI with advanced materials will enable the development of highly efficient and reliable hydrogen sensors, contributing to safer hydrogen storage and utilization in various industries.

**Acknowledgements** This work was supported by the Faculty-development Competitive Research Grants Program of Nazarbayev University for 2024-2026 (Project ref. no. 201223FD8830) "Study of Dopant and Composite Effects on Conducting Polymers' Energy Applications"; Ministry of Education and Science of the Republic of Kazakhstan under project No. BR21882439, "Advancement of the Green Energy: Foundational Research of Solar Fuel Technologies for Sustainable Production and Advanced Storage".

**Author contributions** N.N. and S.A. designed, conceptualized and revised the whole manuscript. P.E. and D.K. wrote the main manuscript text. A.T., K. U., and S.D. wrote the sections and prepared Figs. 1–8 and Table 1–5. All authors reviewed the manuscript.

**Funding** Faculty-development Competitive Research Grants Program of Nazarbayev University (Project ref. no. 201223FD8830); Ministry of Education and Science of the Republic of Kazakhstan (Grant No. BR21882439).

**Data availability** No datasets were generated or analysed during the current study.

## Declarations

**Competing interests** The authors declare that they have no Conflict of interests.

## References

1. Ellis GS, Gelman SE. Model predictions of global geologic hydrogen resources. Sci Adv. 2024. https://doi.org/10.1126/sciadv.ado0955.
2. Sisman O, Erkovan M, Kilinc N Hydrogen sensors for safety applications, First Edit. Elsevier Ltd; 2023.
3. de Kleijne K, Huijbregts MAJ, Knobloch F, et al. Worldwide greenhouse gas emissions of green hydrogen production and transport. Nat Energy. 2024. https://doi.org/10.1038/s41560-024-01563-1.
4. Ponnamma D, Sadasivuni KK, Strankowski M, et al. Eco-friendly electromagnetic interference shielding materials from flexible reduced graphene oxide filled polycaprolactone/polyaniline nanocomposites. Polym Plast Technol Eng. 2016;55:920–8. https://doi.org/10.1080/03602559.2015.1132435.
5. Aizamddin MF, Mahat MM, Zainal Ariffin Z, et al. Antibacterial performance of protonated polyaniline-integrated polyester fabrics. Polymers (Basel). 2022. https://doi.org/10.3390/polym14132617.
6. Jlassi K, Radwan AB, Sadasivuni KK, et al. Anti-corrosive and oil sensitive coatings based on epoxy/polyaniline/magnetite-clay composites through diazonium interfacial chemistry. Sci Rep. 2018;8:13369. https://doi.org/10.1038/s41598-018-31508-0.
7. Sadasivuni KK, Ponnamma D, Kasak P, et al. Designing dual phase sensing materials from polyaniline filled styrene–isoprene–styrene composites. Mater Chem Phys. 2014;147:1029–36. https://doi.org/10.1016/j.matchemphys.2014.06.055.
8. Haynes A, Gouma PI. Perspective—conducting polymer hybrids as diagnostic chemosensors. J Electrochem Soc. 2022;169:037513. https://doi.org/10.1149/1945-7111/ac5baf.
9. Dhand C, Das M, Datta M, Malhotra BD. Recent advances in polyaniline based biosensors. Biosens Bioelectron. 2011;26:2811–21. https://doi.org/10.1016/j.bios.2010.10.017.
10. Pham QM, Kim S. High surface area polyaniline nanofiber synthesized in compressed $CO_2$ and its application to a hydrogen sensor. Korean J Chem Eng. 2016;33:290–8. https://doi.org/10.1007/s11814-015-0122-y.
11. Arsat R, Yu XF, Li YX, et al. Hydrogen gas sensor based on highly ordered polyaniline nanofibers. Sens Actuators, B Chem. 2009;137:529–32. https://doi.org/10.1016/j.snb.2009.01.028.

12. Askar P, Kanzhigitova D, Ospanova A, et al. 1 Ppm-detectable hydrogen gas sensor based on nanostructured polyaniline. Sci Rep. 2024;14:26984. https://doi.org/10.1038/s41598-024-77083-5.
13. Lata KJ, Rana RK. Synthesis and characterization of polyaniline-copper oxide nano-composites. Int J Chem Stud. 2024;12:46–50. https://doi.org/10.22271/chemi.2024.v12.i1a.12396.
14. Choudhury S, Deepak D, Bhattacharya G, et al. MoS2-polyaniline based flexible electrochemical biosensor: toward pH monitoring in human sweat. Macromol Mater Eng. 2023;308:2300007. https://doi.org/10.1002/mame.202300007.
15. Gupta V, Miura N. Electrochemically deposited polyaniline nanowire's network a high-performance electrode material for redox supercapacitor. Electrochem Solid-State Lett. 2005;8:2–5. https://doi.org/10.1149/1.2087207.
16. Kausar A. Polyaniline and quantum dot-based nanostructures: Developments and perspectives. J Plast Film Sheeting. 2020;36:430–47. https://doi.org/10.1177/8756087920926649.
17. Rakhi RB, Chen W, Alshareef HN. Conducting polymer/carbon nanocoil composite electrodes for efficient supercapacitors. J Mater Chem. 2012;22:5177–83. https://doi.org/10.1039/C2JM15740C.
18. Stoppa M, Chiolerio A. Wearable electronics and smart textiles: A critical review. Sensors (Switzerland). 2014;14:11957–92. https://doi.org/10.3390/s140711957.
19. Liao Z, Lin C, Yang C, Jia Y, Wu P, Qiao S. Study on the Preparation and Electrochemical Properties of Nano ZnO/polyaniline Composite Anticorrosive Coating. In2016 International Conference on Advances in Energy, Environment and Chemical Science 2016 May (pp. 294-298). Atlantis Press.
20. Hobaica SC. Stability of polyaniline in air and acidic water. J Polym Sci Part B Polym Phys. 2003;41:807–22. https://doi.org/10.1002/polb.10437.
21. Fratoddi I, Venditti I, Cametti C, Russo MV. Chemiresistive polyaniline-based gas sensors: a mini review. Sens Actuators B Chem. 2015;220:534–48. https://doi.org/10.1016/j.snb.2015.05.107.
22. Kanzhigitova D, Askar P, Tapkharov A, et al. p-Toluenesulfonic acid doped vanadium pentoxide/polypyrrole film for highly sensitive hydrogen sensor. Adv Compos Hybrid Mater. 2023;6:218. https://doi.org/10.1007/s42114-023-00796-0.
23. Kafash S, Milani Moghaddam H. Porous polyaniline tube-like/$TiO_2$ nano-heterostructure for sensing hydrogen gas at environmental conditions. Int J Hydrogen Energy. 2022;47:14740–58. https://doi.org/10.1016/j.ijhydene.2022.02.222.
24. Sadek AZ, Baker CO, Powell DA, et al. Polyaniline nanofiber based surface acoustic wave gas sensors-effect of nanofiber diameter on H2 response. IEEE Sens J. 2007;7:213–8. https://doi.org/10.1109/JSEN.2006.883769.
25. Jamnani SR, Moghaddam HM, Leonardi SG, Neri G. PANI/$Sm_2O_3$ nanocomposite sensor for fast hydrogen detection at room temperature. Synth Met. 2020;268:116493. https://doi.org/10.1016/j.synthmet.2020.116493.
26. Gawli Y, Banerjee A, Dhakras D, et al. 3D Polyaniline architecture by concurrent inorganic and organic acid doping for superior and robust high rate supercapacitor performance. Sci Rep. 2016. https://doi.org/10.1038/srep21002.
27. Ouyang J. Recent advances of intrinsically conductive polymers. Wuli Huaxue Xuebao/ Acta Phys - Chim Sin. 2018;34:1211–20. https://doi.org/10.3866/PKU.WHXB201804095.
28. Virji S, Kaner RB, Weiller BH. Hydrogen sensors based on conductivity changes in polyaniline nanofibers. J Phys Chem B. 2006;110:22266–70. https://doi.org/10.1021/jp063166g.
29. Al-Mashat L, Shin K, Kalantar-Zadeh K, et al. Graphene/polyaniline nanocomposite for hydrogen sensing. J Phys Chem C. 2010;114:16168–73. https://doi.org/10.1021/jp103134u.
30. Fowler JD, Virji S, Kaner RB, Weiller BH. Hydrogen detection by Polyaniline nanofibers on gold and platinum electrodes. J Phys Chem C. 2009;113:6444–9. https://doi.org/10.1021/jp810500q.
31. Koo WT, Cho HJ, Kim DH, et al. Chemiresistive hydrogen sensors: fundamentals, recent advances, and challenges. ACS Nano. 2020;14:14284–322. https://doi.org/10.1021/acsnano.0c05307.
32. Shin W, Matsumiya M, Izu N, Murayama N. Hydrogen-selective thermoelectric gas sensor. Sens Actuators, B Chem. 2003;93:304–8. https://doi.org/10.1016/S0925-4005(03)00225-9.
33. Shah MA, Lee DG, Lee BY, Hur S. Classifications and applications of inkjet printing technology: a review. IEEE Access. 2021;9:140079–102. https://doi.org/10.1109/ACCESS.2021.3119219.
34. Liu N, Sheng X, Zhang M, et al. Squeeze-type piezoelectric inkjet printhead actuating waveform design method based on numerical simulation and experiment. Micromachines. 2022. https://doi.org/10.3390/mi13101695.
35. Le DD, Nguyen TNN, Doan DCT, et al. Fabrication of interdigitated electrodes by inkjet printing technology for apllication in ammonia sensing. Adv Nat Sci Nanosci Nanotechnol. 2016. https://doi.org/10.1088/2043-6262/7/2/025002.
36. Crowley K, Morrin A, Shepherd RL, et al. Fabrication of polyaniline-based gas sensors using piezoelectric inkjet and screen printing for the detection of hydrogen sulfide. IEEE Sens J. 2010;10:1419–26. https://doi.org/10.1109/JSEN.2010.2044996.
37. Abuzalat O, Wong D, Park SS, Kim S. High-performance, room temperature hydrogen sensing with a Cu-BTC/polyaniline nanocomposite film on a quartz crystal microbalance. IEEE Sens J. 2019;19:4789–95. https://doi.org/10.1109/JSEN.2019.2904870.
38. Bavili N, Balkan T, Morova B, et al. Highly sensitive optical sensor for hydrogen gas based on a polymer microcylinder ring resonator. Sens Actuators, B Chem. 2020;310:127806. https://doi.org/10.1016/j.snb.2020.127806.
39. Lee JS, Kim SG, Cho S, Jang J. Porous palladium coated conducting polymer nanoparticles for ultrasensitive hydrogen sensors. Nanoscale. 2015;7:20665–73. https://doi.org/10.1039/c5nr06193h.
40. Mirzaei A, Kumar V, Bonyani M, et al. Conducting polymer nanofibers based sensors for organic and inorganic gaseous compounds. Asian J Atmos Environ. 2020;14:85–104. https://doi.org/10.5572/ajae.2020.14.2.85.
41. Huang J, Virji S, Weiller BH, Kaner RB. Nanostructured polyaniline sensors. Chem - A Eur J. 2004;10:1314–9. https://doi.org/10.1002/chem.200305211.
42. Cheung JH, Stockton WB, Rubner MF. Molecular-level processing of conjugated polymers. 3. Layer-by-layer manipulation of polyaniline via electrostatic interactions. Macromolecules. 1997;30:2712–6. https://doi.org/10.1021/ma970047d.
43. Ferreira M, Onitsuka O, Stockton WB, Rubner MF (1997) Self-assembled heterostructures of electroactive polymers: new opportunities for thin-film devices. In: Photonic and Optoelectronic Polymers. American Chemical Society, pp 29–437

44. Yang Z, Peng H, Wang W, Liu T. Crystallization behavior of poly(ε-caprolactone)/layered double hydroxide nanocomposites. J Appl Polym Sci. 2010;116:2658–67. https://doi.org/10.1002/app.
45. Bhadra S, Singha NK, Khastgir D. Dual functionality of PTSA as electrolyte and dopant in the electrochemical synthesis of polyaniline, and its effect on electrical properties. Polym Int. 2007;56:919–27. https://doi.org/10.1002/pi.2225.
46. Mahato N, Jang H, Dhyani A, Cho S. Recent progress in conducting polymers for hydrogen storage and fuel cell applications. Polymers. 2020;12:2480.
47. Kanzhigitova D, Abutalip M, Nazir F, et al. Controlled synthesis of polyaniline-based nanomaterials with self-assembly and interface manipulation. Langmuir. 2023. https://doi.org/10.1021/acs.langmuir.3c03167.
48. Abutalip M, Zhigerbayeva G, Kanzhigitova D, et al. Strategic synthesis of 2D and 3D conducting polymers and derived nanocomposites. Adv Mater. 2022;2208864:1–8. https://doi.org/10.1002/adma.202208864.
49. Xue Y, Chen S, Yu J, et al. Nanostructured conducting polymers and their composites: synthesis methodologies, morphologies and applications. J Mater Chem C. 2020;8:10136–59. https://doi.org/10.1039/d0tc02152k.
50. Dan LI, Huang J, Kaner RB. Polyaniline nanofibers: a unique polymer nanostructure for versatile applications. Acc Chem Res. 2009;42:135–45. https://doi.org/10.1021/ar800080n.
51. Pang Z, Yildirim E, Pasquinelli MA, Wei Q. Ammonia sensing performance of polyaniline-coated polyamide 6 nanofibers. ACS Omega. 2021;6:8950–7. https://doi.org/10.1021/acsomega.0c06272.
52. Sharma HJ, Sonwane ND, Kondawar SB. Electrospun $SnO_2$/Polyaniline composite nanofibers based low temperature hydrogen gas sensor. Fibers Polym. 2015;16:1527–32. https://doi.org/10.1007/s12221-015-5222-0.
53. Febrina M, Rianjanu A, Rajak A, et al. Electrospun polyacrylonitrile nanofibers mixed with citric acid as a quartz crystal microbalance ammonia vapor sensor. ChemistrySelect. 2022;7:1–5. https://doi.org/10.1002/slct.202103615.
54. Liu J, Cui N, Xu Q, et al. High-performance PANI-based ammonia gas sensor promoted by surface nanostructuralization. ECS J Solid State Sci Technol. 2021;10:027007. https://doi.org/10.1149/2162-8777/abe3ce.
55. Joulazadeh M, Navarchian AH. Alcohol sensibility of one-dimensional polyaniline and polypyrrole nanostructures. IEEE Sens J. 2015;15:1697–704. https://doi.org/10.1109/JSEN.2014.2360915.
56. Zou Y, Wang Q, Xiang C, et al. Doping composite of polyaniline and reduced graphene oxide with palladium nanoparticles for room-temperature hydrogen-gas sensing. Int J Hydrogen Energy. 2016;41:5396–404. https://doi.org/10.1016/j.ijhydene.2016.02.023.
57. Tang CC, Huang R, Long Y-Z, et al. Synthesis, structural and gas sensing properties of nano-branched coaxial polyaniline fibers by electrospinning. Adv Mater Res. 2012;562–564:308–11. https://doi.org/10.4028/www.scientific.net/AMR.562-564.308.
58. Shrivastava S, Mathur S, Sharma N, et al. Effect of MWNT concentration on hydrogen gas sensing property of MWNT-ployaniline composite. Int J Hydrogen Energy. 2023;48:38107–17. https://doi.org/10.1016/j.ijhydene.2022.12.053.
59. Bafandeh N, Solaymani S, Sabbaghzadeh J, et al. Carbon nanotubes/polyaniline as hydrogen gas sensor: optical bandgap, micro-morphology, and skin depth studies. AIP Adv. 2023. https://doi.org/10.1063/5.0141597.
60. Chen W, Rakhi RB, Alshareef HN. Morphology-dependent enhancement of the pseudocapacitance of template-guided tunable polyaniline nanostructures. J Phys Chem C. 2013;117:15009–19. https://doi.org/10.1021/jp405300p.
61. Xiong S, Zhang Y, Wang Y, et al. Comparative study on the supercapacitive properties of PANI nanofibers, nanotubes, and nanospheres. High Perform Polym. 2020;32:600–8. https://doi.org/10.1177/0954008319890644.
62. Huang J, Virji S, Weiller BH, Kaner RB. Polyaniline nanofibers: facile synthesis and chemical sensors. J Am Chem Soc. 2003;125:314–5. https://doi.org/10.1021/ja028371y.
63. Qin A, Lam JWY, Tang BZ. Click polymerization. Chem Soc Rev. 2010;39:2522–44. https://doi.org/10.1039/b909064a.
64. Pan L, Yu G, Zhai D, Lee HR, Zhao W, Liu N, Wang H, Tee BC, Shi Y, Cui Y, Bao Z. Hierarchical nanostructured conducting polymer hydrogel with high electrochemical activity. Proc Nat Acad Sci. 2012;109(24):9287–92. https://doi.org/10.1073/pnas.1202636109/-/DCSupplemental.
65. Rana DS, Kalia S, Kumar R, et al. Two-dimensional layered reduced graphene oxide-tungsten disulphide nanocomposite for highly sensitive and selective determination of para nitrophenol. Environ Nanotechnol Monit Manag. 2022;18:100724. https://doi.org/10.1016/j.enmm.2022.100724.
66. Kalia S, Rana DS, Thakur N, et al. Two-dimensional layered molybdenum disulfide ($MoS_2$)-reduced graphene oxide (rGO) heterostructures modified with $Fe_3O_4$ for electrochemical sensing of epinephrine. Mater Chem Phys. 2022;287:126274. https://doi.org/10.1016/j.matchemphys.2022.126274.
67. Murugesan T, Kumar RR, Anbalagan AK, et al. Interlinked polyaniline/ZnO nanorod composite for selective $NO_2$Gas sensing at room temperature. ACS Appl Nano Mater. 2022;5:4921–30. https://doi.org/10.1021/acsanm.1c04519.
68. Sharma S, Kumar R, Yadav RM. Polyacrylonitrile/N-doped graphene quantum dots nanocomposite activity as SERS nanosensors for detection of methylene blue. Mater Today Commun. 2023;36:106860. https://doi.org/10.1016/j.mtcomm.2023.106860.
69. Zhang Y, Zhuang X, Su Y, et al. Polyaniline nanosheet derived B/N co-doped carbon nanosheets as efficient metal-free catalysts for oxygen reduction reaction. J Mater Chem A. 2014;2:7742–6. https://doi.org/10.1039/c4ta00814f.
70. Rana DS, Kalia S, Kumar R, et al. Microwave-assisted facile synthesis of layered reduced graphene oxide-tungsten disulfide sandwiched $Fe_3O_4$ nanocomposite as effective and sensitive sensor for detection of dopamine. Mater Chem Phys. 2022;287:126283. https://doi.org/10.1016/j.matchemphys.2022.126283.
71. Maegawa K, Nagai H, Kumar R, et al. Development of polybenzimidazole modification with open-edges/porous-reduced graphene oxide composite membranes for excellent stability and improved PEM fuel cell performance. Mater Chem Phys. 2023;294:126994. https://doi.org/10.1016/j.matchemphys.2022.126994.
72. Rana DS, Kalia S, Thakur N, et al. Synthesis of reduced graphene oxide-molybdenum disulfide nanocomposite as potential scaffold for fabrication of efficient hydrazine sensor. Mater Chem Phys. 2023;294:127048. https://doi.org/10.1016/j.matchemphys.2022.127048.
73. Kumar R, Dias W, Rubira RJG, et al. Simple and fast approach for synthesis of reduced graphene oxide–$MoS_2$ hybrids for room temperature gas detection. IEEE Trans Electron Dev. 2018;65:3943–9. https://doi.org/10.1109/TED.2018.2851955.
74. Babel V, Hiran BL. A review on polyaniline composites: synthesis, characterization, and applications. Polym Compos. 2021;42:3142–57. https://doi.org/10.1002/pc.26048.

75. Zhang W, Cao S, Wu Z, Zhang M, Cao Y, Guo J, Zhong F, Duan H, Jia D. High-performance gas sensor of polyaniline / carbon nanotube composites promoted by. Sensors. 2019;20:149.
76. Wang K, Meng Q, Zhang Y, et al. High-performance two-ply yarn supercapacitors based on carbon nanotubes and polyaniline nanowire arrays. Adv Mater. 2013;25:1494–8. https://doi.org/10.1002/adma.201204598.
77. Yadav AK, Mohammad N, Chamanehpour E, et al. Polyaniline (PANI) nanocomposites with Se Te and their metal chalcogenides: a review. RSC Appl Polym. 2024. https://doi.org/10.1039/d4lp00093e.
78. Badry R, Elhaes H, Ibrahim A, et al. Investigating the electronic properties and reactivity of polyaniline emeraldine base functionalized with metal oxides. Sci Rep. 2024;14:27024. https://doi.org/10.1038/s41598-024-72435-7.
79. Bafandeh N, Larijani MM, Shafiekhani A. Investigation on hydrogen sensing property of MWCNT/Pani nanocomposite films. Polym Bull. 2020;77:3697–706. https://doi.org/10.1007/s00289-019-02915-8.
80. Wu Z, Chen X, Zhu S, et al. Enhanced sensitivity of ammonia sensor using graphene/polyaniline nanocomposite. Sens Actuators, B Chem. 2013;178:485–93. https://doi.org/10.1016/j.snb.2013.01.014.
81. Yan Y, Yang G, Xu JL, et al. Conducting polymer-inorganic nanocomposite-based gas sensors: a review. Sci Technol Adv Mater. 2020;21:768–86. https://doi.org/10.1080/14686996.2020.1820845.
82. Jia A, Liu B, Liu H, et al. Interface design of $SnO_2$@PANI nanotube with enhanced sensing performance for ammonia detection at room temperature. Front Chem. 2020;8:1–9. https://doi.org/10.3389/fchem.2020.00383.
83. Farooqi BA, Yar M, Ashraf A, et al. Remarkable enhancement in sensor ability of polyaniline upon composite formation with ZnO for industrial effluents. J Mol Graph Model. 2020;101:107724. https://doi.org/10.1016/j.jmgm.2020.107724.
84. Pippara RK, Chauhan PS, Yadav A, et al. Room temperature hydrogen sensing with polyaniline/$SnO_2$/Pd nanocomposites. Micro Nano Eng. 2021;12:100086. https://doi.org/10.1016/j.mne.2021.100086.
85. Venkatesh E, Singh S, Tripathy S, Singh SG. Amorphous-Carbon/Si heterojunction device for room-temperature NH 3 sensing. IEEE Sens Lett. 2018;3(2):1–4.
86. Mashao G, Ramohlola KE, Mdluli SB, et al. Zinc-based zeolitic benzimidazolate framework/polyaniline nanocomposite for electrochemical sensing of hydrogen gas. Mater Chem Phys. 2019;230:287–98. https://doi.org/10.1016/j.matchemphys.2019.03.079.
87. Srivastava S, Kumar S, Singh VN, et al. Synthesis and characterization of $TiO_2$ doped polyaniline composites for hydrogen gas sensing. Int J Hydrog Energy. 2011;36:6343–55. https://doi.org/10.1016/j.ijhydene.2011.01.141.
88. Nasirian S, Milani Moghaddam H. Effect of different titania phases on the hydrogen gas sensing features of polyaniline/$TiO_2$ nanocomposite. Polymer (Guildf). 2014;55:1866–74. https://doi.org/10.1016/j.polymer.2014.02.030.
89. Milani Moghaddam H, Nasirian S. Hydrogen gas sensing feature of polyaniline/titania (rutile) nanocomposite at environmental conditions. Appl Surf Sci. 2014;317:117–24. https://doi.org/10.1016/j.apsusc.2014.08.062.
90. Srivastava S, Kumar S, Vijay YK. Preparation and characterization of tantalum/polyaniline composite based chemiresistor type sensor for hydrogen gas sensing application. Int J Hydrog Energy. 2012;37:3825–32. https://doi.org/10.1016/j.ijhydene.2011.04.155.
91. Arora K, Puri NK. Chemiresistive sensing platform based on PdO-PANI/ITO heterostructure for room temperature hydrogen detection. Mater Chem Phys. 2020;247:122850. https://doi.org/10.1016/j.matchemphys.2020.122850.
92. More AM, Sharma HJ, Kondawar SB, Dongre SP. Journal of Materials NanoScience Ag-$SnO_2$ /Polyaniline composite nanofibers for low operating temperature hydrogen gas sensor. J Mater Nanosci J Mat NanoSci. 2017;4:13–8.
93. Sharma HJ, Jamkar DV, Kondawar SB. Electrospun nanofibers of conducting polyaniline/Al-$SnO_2$ composites for hydrogen sensing applications. Proc Mater Sci. 2015;10:186–94. https://doi.org/10.1016/j.mspro.2015.06.040.
94. Enachi M, Lupan O, Braniste T, et al. Integration of individual $TiO_2$ nanotube on the chip: nanodevice for hydrogen sensing. Phys Status Solidi - Rapid Res Lett. 2015;9:171–4. https://doi.org/10.1002/pssr.201409562.
95. Nasirian S, Milani Moghaddam H. Hydrogen gas sensing based on polyaniline/anatase titania nanocomposite. Int J Hydrog Energy. 2014;39:630–42. https://doi.org/10.1016/j.ijhydene.2013.09.152.
96. Darmadi I, Nugroho FAA, Langhammer C. High-performance nanostructured palladium-based hydrogen sensors - current limitations and strategies for their mitigation. ACS Sens. 2020;5:3306–27. https://doi.org/10.1021/acssensors.0c02019.
97. Mirzaei A, Yousefi HR, Falsafi F, et al. An overview on how Pd on resistive-based nanomaterial gas sensors can enhance response toward hydrogen gas. Int J Hydrog Energy. 2019;44:20552–71. https://doi.org/10.1016/j.ijhydene.2019.05.180.
98. Cho S, Lee JS, Jun J, Jang J. High-sensitivity hydrogen gas sensors based on Pd-decorated nanoporous poly(aniline-co-aniline-2-sulfonic acid):poly(4-styrenesulfonic acid). J Mater Chem A. 2014;2:1955–66. https://doi.org/10.1039/c3ta13741d.
99. Liu X, Zheng W, Kumar R, et al. Conducting polymer-based nanostructures for gas sensors. Coord Chem Rev. 2022;462:214517. https://doi.org/10.1016/j.ccr.2022.214517.
100. Sharma HJ. $H_2$ and CO gas sensor from $SnO_2$/polyaniline composite nanofibers fabricated by electrospinning. Adv Mater Proc. 2017;2:61–6. https://doi.org/10.5185/amp.2017/114.
101. Kroutil J, Laposa A, Povolny V, et al. Gas sensor with different morphology of PANI layer. Sensors. 2023. https://doi.org/10.3390/s23031106.
102. Han MG, Lee YJ, Byun SW, Im SS. Physical properties and thermal transition of polyaniline film. Synth Met. 2001;124:337–43. https://doi.org/10.1016/S0379-6779(01)00369-1.
103. Turkten N, Karatas Y, Bekbolet M. Preparation of pani modified zno composites via different methods: structural, morphological and photocatalytic properties. Water (Switzerland). 2021. https://doi.org/10.3390/w13081025.
104. Virji S, Huang J, Kaner RB, Weiller BH. Polyaniline nanofiber gas sensors: examination of response mechanisms. Nano Lett. 2004;4:491–6. https://doi.org/10.1021/nl035122e.